Molecular cloning and expression of a chloride channel-associated protein pI_{Cln} in human young red blood cells: association with actin

Robert S. SCHWARTZ[1], Anne C. RYBICKI and Ronald L. NAGEL

Division of Hematology, Albert Einstein College of Medicine–Montefiore Medical Center, 111 East 210th Street, Bronx, NY 10467, U.S.A.

We report the cloning and sequencing from human reticulocytes of cDNA coding for the Cl^- channel-associated protein, pI_{Cln}. Human reticulocyte pI_{Cln} ($HRpI_{Cln}$) cDNA encodes a protein (predicted molecular mass 26293 Da) identical with human non-pigmented ciliary epithelial cell pI_{Cln}. By using full-length $HRpI_{Cln}$ cDNA (approx. 1.2 kb) to probe human lymphocyte metaphase-chromosome spreads, the location of the human I_{Cln} gene was mapped to 11q13 by fluorescence *in situ* hybridization analysis. Polyclonal antibodies to recombinant $HRpI_{Cln}$ detected bands at approx. 43 kDa and approx. 37 kDa in both normal (AA) and sickle (SS) red blood cell (RBC) ghost membranes. In SS ghosts, and in ghosts from a patient with autoimmune haemolytic anaemia with 9.8 % reticulocytes, the amount of $HRpI_{Cln}$ was increased compared with AA ghosts, suggesting that the expression or membrane assembly of $HRpI_{Cln}$ is cell age-dependent. Laser scanning confocal fluorescent microscopy immunolocalized $HRpI_{Cln}$ largely to the RBC membrane. The increased staining intensity of $HRpI_{Cln}$ in a reticulocyte-enriched AA RBC density-separated fraction is consistent with a dependence of $HRpI_{Cln}$ membrane content on cell age. $HRpI_{Cln}$ and β-actin form stable complexes *in vivo*, demonstrated with the yeast two-hybrid system. Low-ionic-strength extraction of ghost membranes, which results in the extraction of the spectrin–actin cytoskeleton, also results in the extraction of $HRpI_{Cln}$, consistent with the possibility for the association of these proteins in RBCs *in vivo*. The results presented here establish the presence of the Cl^- channel-associated protein, pI_{Cln}, in human RBCs, and raises the possibility that this protein has a role in RBC Cl^- transport and volume regulation in young RBCs. Moreover the association of RBC pI_{Cln} with actin offers a model in which to test interactions between RBC ion channels and the cytoskeleton.

INTRODUCTION

Young circulating red blood cells (RBCs) are exposed *in vivo* to acidic conditions, which causes them to take up cations and water and to swell [1–4]. To maintain normal cell volume these young and immature human RBCs, like many mammalian cells, have volume regulatory pathways that include the swelling-induced activation of volume regulatory ion-transport pathways. Transport pathways that are activated by cell swelling and result in salt and water loss are classified as regulatory volume decrease (RVD) pathways. In young and immature human RBCs, a major recognized RVD pathway is the K:Cl co-transporter, in which both K^+ and Cl^- are obligatorily transported [5–8]. K:Cl co-transport activity decreases sharply with reticulocyte maturation, and is very low in normal (AA) adult circulating RBCs [9]. Swelling-activated Cl^- and K^+ channels participate in the RVD response in many different types of non-erythroid cells [10], but these channels have not been described in mammalian RBCs. It has been assumed that Cl^- transport through Cl^- channels would necessarily be a minor pathway in human RBCs owing to the high permeability to Cl^- resulting from the activity of the anion-exchange protein (AE1, band 3) [11]. However, human RBC AE1 is not known to be activated by cell swelling [12] and is thus unlikely to participate in swelling-activated RVD.

We report here the cloning, sequencing, chromosomal location and immunolocalization of the Cl^- channel-associated protein, pI_{Cln}, in human RBCs, and demonstrate its association with β-actin *in vivo*. Our findings raise the possibility that RBC pI_{Cln} has a role in Cl^- transport, RVD and/or volume-sensing pathways in young and immature RBCs, and that interactions between pI_{Cln} and the cytoskeleton are involved in regulating these activities.

EXPERIMENTAL

Blood

Samples were obtained, after informed consent, by venipuncture from haematologically normal adult volunteers (AA), from adult patients with sickle cell anaemia (SS) who had been transfusion-free for a minimum of 3 months, and from a patient with a provisional diagnosis of autoimmune haemolytic anaemia [66-year-old female, Coombs positive, normocellular marrow (40 %), no history of transfusions, haemoglobin (Hb) 9.0 g/dl, mean corpuscular volume 91 fl, haematocrit 29 %, reticulocytes 9.8 %]. Blood samples were collected in acid–citrate–dextrose-anticoagulated tubes. If the blood was not used immediately it was stored at 4 °C and used within 24 h. For some experiments, AA RBCs were separated into density fractions on Larex–Percoll continuous density gradients [13] and the light density fraction (less than 1.07 g/ml) enriched in reticulocytes was removed, the RBCs were washed in PBS, pH 8, and used for immunocytochemistry studies (see below).

Preparation of RBC ghost membranes

Acid–citrate–dextrose-anticoagulated blood was centrifuged at 1500 ***g*** for 5 min at 4 °C and the plasma and buffy coat were discarded. The RBC pellet was resuspended in 10 vol. of PBS,

Abbreviations used: AD, activation domain; BD, binding domain; FISH, fluorescence *in situ* hybridization; GST, glutathione S-transferase; Hb, haemoglobin; $HRpI_{cln}$, human reticulocyte pI_{cln}; NPE, non-pigmented ciliary epithelial cell; ORF, open reading frame; RBC, red blood cell; RVD, regulatory volume decrease.

[1] To whom correspondence should be addressed.

Table 1 Oligonucleotide PCR primers used for $HRpI_{Cln}$ cDNA sequencing and generation of recombinant $HRpI_{cln}$ and recombinant β-actin

Primers 1, 2, 4, 6, 8, 9, 11, 13 and 14 were used for $HRpI_{Cln}$ sequencing. Primers 8 and 9 were used for generating recombinant $HRpI_{Cln}$. Primers 15 and 16 were used for generating recombinant β-actin.

Oligonucleotide	Sequence (5′ → 3′)	Position in $HRpI_{Cln}$	Direction (5′ → 3′)
1	AGCTTCCTCAAAAGTTTCCCG	4	→
2	GTGATCAACATCTGCATCCTC	691	←
4	ACATGCATTATCCAGGGACCG	189	→
6	ATGAAGATGGGATGGAGGTGG	641	→
8	CTTTGAGGACTTCATCCCAGA	1269*	←
9	TCAGGGCCTGTGTTGCCGCA	−30	→
11	GACAGGGGGACATCCCTACAT	479	→
13	CGGTCCCTGGATAATGCATGT	189	←
14	CAGCAGAAGATAGATAATATGA	878	→
Oligonucleotide	**Sequence (5′ → 3′)**	**Position in β-actin†**	**Direction (5′ → 3′)**
15	AGCACAGAGCCTCGCCTTTG	−58	→
16	ACTGCTGTCACCTTCACCGTT	1352	←

* Position in NPE pI_{Cln} (Genbank/EMBL accession number U17899).
† Human β-actin (GenBank/EMBL accession number X63432).

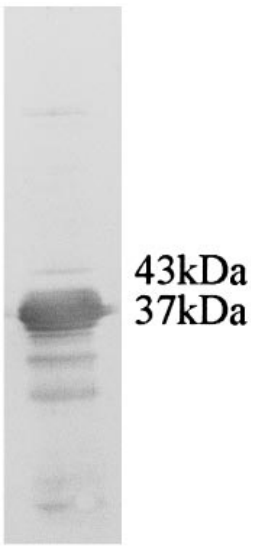

Figure 1 Recombinant GST–$HRpI_{Cln}$ fusion protein was generated with pGEX-KG plasmid [19]

GST–$HRpI_{Cln}$ fusion protein in the bacterial lysate was affinity-purified with glutathione–agarose, and $HRpI_{Cln}$ was cleaved from the fusion protein with thrombin. $HRpI_{Cln}$ (10 μg) was subjected to reducing SDS/PAGE [12% (w/v) gel] [20] and transferred electrophoretically to nitrocellulose [21]. The nitrocellulose was probed with rabbit polyclonal anti-MDCK pI_{Cln} (aFPA [22], 5 μg/ml). Antibody binding was detected by using alkaline phosphatase-conjugated anti-(rabbit IgG) and alkaline phosphatase colour-developing reagents.

RBCs were collected as above and washed a further three times in PBS, and were subjected to hypotonic lysis in 5 mM phosphate buffer, pH 8.0 (5P8) [14]. The resulting ghost membranes were collected by centrifugation at 20000 ***g*** for 20 min at 4 °C and washed a further three times in 5P8. The ghosting buffer also contained 0.4 mM di-isopropyl fluorophosphate and 0.5 mM EGTA to inhibit proteolysis.

RNA and cDNA preparation and cDNA sequencing

Reticulocyte total RNA was isolated from SS RBCs, because SS patients typically have elevated reticulocyte levels owing to ongoing haemolysis [15]. Total RNA was isolated by isotonic lysis, acid titration and organic solvent extraction [16], and used as the template for reverse transcription into cDNA. cDNA was amplified by PCR with oligonucleotide primers complementary to regions of human non-pigmented ciliary epithelial cell (NPE) pI_{Cln} [17] (Table 1). The PCR products were subcloned into the pCR2.1 plasmid (Invitrogen, San Diego, CA, U.S.A.), in accordance with the manufacturer's instructions, and double-stranded mini-prep plasmid DNA was sequenced with Sequenase version 2.0 (US Biochemical, Cleveland, OH, U.S.A.). The sequencing primers were identical with those used for PCR amplification (Table 1).

Chromosomal localization

Metaphase spreads were prepared from normal human lymphocytes by routine cytogenetic procedures. Full-length human reticulocyte pI_{Cln} ($HRpI_{Cln}$) cDNA (approx. 1.2 kb), used to probe the metaphase spreads, was generated from human reticulocyte cDNA by PCR with oligonucleotide primers 8 and 9 (Table 1) and the DNA was labelled with biotin-14-dATP, with a Bio-Nick labelling kit (Gibco/BRL, Gaithersburg, MD, U.S.A.). Unincorporated nucleotides were separated from the probe by passing the labelled probe through a Quick spin column (Boehringer Mannheim, Indianapolis, IN, U.S.A.). Specific chromosomes were identified by Geimsa staining. Fluorescence *in situ* hybridization (FISH) was performed as described previously [18] in the Albert Einstein College of Medicine Cytogenetics Shared Resource Facility by using FITC-conjugated avidin (Oncor, Gaithersburg, MD, U.S.A.) to detect the biotin-labelled probe. Analysis of FISH results was performed with a Bio-Rad laser-sharp MRC confocal scanner (Bio-Rad, Hercules, CA, U.S.A.).

Generation of recombinant $HRpI_{Cln}$ and production of polyclonal antibody

Polyclonal anti-$HRpI_{Cln}$ antibody was generated in rabbits from recombinant glutathione S-transferase (GST)–$HRpI_{Cln}$ fusion protein with the pGEX-KG plasmid in *Escherichia coli* [19]. GST–$HRpI_{Cln}$ fusion protein in the bacterial lysate was affinity-purified with glutathione agarose (Pharmacia, Piscataway, NJ, U.S.A.) and $HRpI_{Cln}$ was cleaved from the GST–$HRpI_{Cln}$ fusion protein with thrombin (Sigma Chemical Co., St. Louis, MO, U.S.A.) [19]. The thrombin-cleaved $HRpI_{Cln}$ migrated as a major band at approx. 37 kDa on denaturing SDS/PAGE [20], as determined by an analysis of Coomassie Blue-stained gels (results not shown). Analysis of the $HRpI_{Cln}$ by Western blotting [21] with polyclonal anti-MDCK pI_{Cln} (aFPA [22]) revealed an additional minor band at approx. 43 kDa (Figure 1). IgG was affinity-purified from immune rabbit serum with Protein A–Sepharose 4B beads (Bio-Rad), in accordance with the manufacturer's instructions.

Immunocytochemistry

A 20 μl sample of a 0.3% haematocrit of washed AA RBCs was layered on wells of 10 mm × 5 mm printed glass slides (Roboz Surgical Instrument Co.) and air-dried. The air-dried cells were

fixed in methanol (10 min at −20 °C) followed by membrane permeabilization in acetone (1 min at −20 °C) and further washing in PBS (three times, 5 min each, at room temperature). Non-specific antibody-binding sites were blocked with 6 % (v/v) goat serum (Sigma cat. no. G9023) in PBS for a minimum of 2 h at room temperature, followed by rinsing with PBS and then incubating with polyclonal anti-pI_{Cln} antibody (both anti-MDCK pI_{Cln} [22] and anti-$HRpI_{Cln}$ antibody were used, diluted in 6 % goat serum/PBS to 2 and 20 μg/ml respectively) or with non-immune rabbit IgG (20 μg/ml in 6 % goat serum/PBS), for 18 h at 4 °C in a humidified chamber. After the incubation the cells were washed twice with PBS containing 0.2 % Triton X-100, followed by washing twice with PBS. Bound antibody was detected by incubating the cells for 1 h at room temperature with biotinylated anti-rabbit IgG (Sigma cat. no. B8895, diluted 1:500 in 6 % goat serum/PBS). The cells were then washed as above and incubated for 30 min at room temperature with FITC-conjugated ExtraAvidin (Sigma cat. no. E2761, diluted 1:167 in PBS), followed by three washes with PBS containing 0.2 % Triton X-100. The cells were air-dried and glass cover slips were applied with mounting medium (Sigma cat. no. 100-4). Cells were imaged with a confocal laser scanning microscope system (Bio-Rad) equipped with phase contrast and epifluorescence objectives.

Yeast two-hybrid system

Fusion proteins were constructed containing full-length $HRpI_{Cln}$ and full-length β-actin as follows: $HRpI_{Cln}$ [complete open reading frame (ORF) cDNA generated by PCR with primers 8 and 9 in Table 1] was cloned into vector pAS2-1, which contains the GAL4-binding domain (BD) (Matchmaker kit; Clontech, Palo Alto, CA, U.S.A.); β-actin (complete ORF cDNA generated by PCR with primers 15 and 16 in Table 1) cDNA was cloned into vector pACT2, which contains the GAL4 activation domain (AD). To test for intracellular protein–protein interaction, BD and AD plasmids, alone or together, were used to transform yeast strain Y187. After selection of co-transformants in yeast selection media (−tryptophan, −leucine), colonies were assayed for β-galactosidase activity with *o*-nitrophenyl β-D-galactoside (ONPG; Sigma cat. no. N1127) as follows: an overnight yeast culture (from one colony) was grown to mid-exponential phase (3–5 h at 30 °C), the D_{600} was recorded, the yeast were lysed in liquid N_2, and ONPG was added. After an appropriate time allowed for colour development, the reaction was terminated and the A_{420} of the cell supernatant was recorded. β-Galactosidase units are defined as $1000\,A_{420}/(tvD_{600})$, where t is time of incubation, v is 0.1 ml × concentration factor and D_{600} is the attenuance of 1 ml of yeast culture at 600 nm.

RESULTS

pI_{Cln} cDNA cloning and sequencing

Human reticulocyte cDNA was generated from total RNA by reverse transcription–PCR, and the cDNA was amplified with a series of PCR oligonucleotide primer pairs designed to allow the amplification of the entire human NPE pI_{Cln} [17] (Genbank/EMBL accession number U17899) ORF and portions of the 5′ and 3′ untranslated regions. $HRpI_{Cln}$ was 100 % identical with NPE pI_{Cln} in the ORF, and also in the first 30 bases of the 5′ untranslated region and in 471 bases of the 3′ untranslated region, with the single exception at nt 781 in the $HRpI_{Cln}$ 3′ untranslated region that was T as opposed to G in NPE pI_{Cln}. The predicted $HRpI_{Cln}$ protein sequence is 100 % identical with NPE pI_{Cln}, and codes for 237 amino acids with a predicted

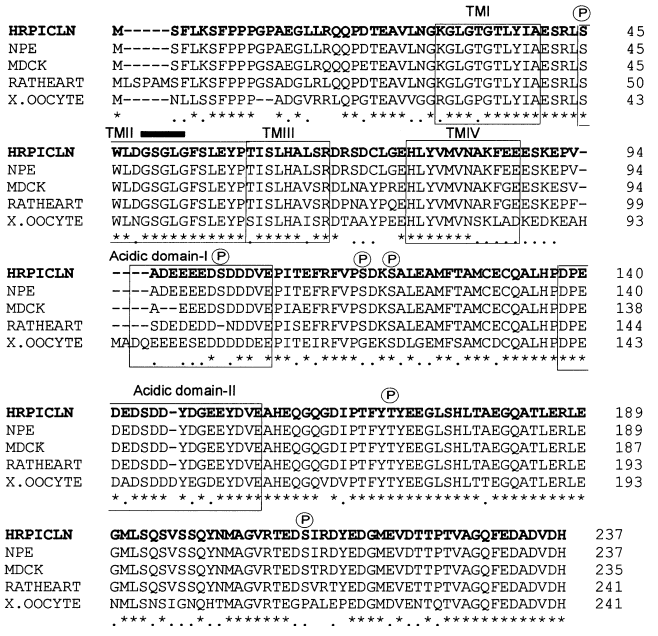

Figure 2 Sequence alignment of pI_{Cln} homologues

Deduced amino acid sequences of pI_{Cln} from human reticulocytes (HRPICLN), human NPE cells (NPE, GenBank/EMBL accession number U17899), dog kidney epithelia (MDCK, EMBL sequence CCCC), rat atria (RATHEART, EMBL sequence RNICLNA) and *Xenopus* oocytes (X. OOCYTE, EMBL sequence XLICLNA). Alignment was made with the CLUSTAL program in PCGENE (version 6.85, IntelliGenetics, Campbell, CA, U.S.A.). Amino acids are shown in single-letter code. Boxed areas indicate four predicted transmembrane β-sheets (TMI to TMIV, from [23]) and two acidic amino acid-enriched domains (acidic domains I and II, from [23]). The solid rectangle indicates the position of the putative nucleotide-binding site (from [23]). Symbols: Ⓟ, consensus protein kinase C phosphorylation sites (Ser^{117} and Ser^{210}) and consensus casein kinase II phosphorylation sites (Ser^{45}, Ser^{102}, Ser^{120}, Thr^{169} and Ser^{210}), determined with PROSITE (version 1.2 in PCGENE, see above); asterisk, identical amino acid; full point, conservative amino acid substitution.

molecular mass of 26293 Da (Figure 2). Overall protein identity with pI_{Cln} from other tissues and species is 65 % (88 % similarity including conservative substitutions). The four putative transmembrane β-sheet domains (TMI, residues 30–40; TMII, residues 49–59; TMIII, residues 60–68; TMIV, residues 77–88) are 100 % conserved (including conservative amino acid substitutions) across all tissues and species so far sequenced, with domain TMIV having the most conservative substitutions (5 of 12 residues) (Figure 2). There are two consensus protein kinase C phosphorylation sites at Ser^{117} and Ser^{210}, and five consensus casein kinase II phosphorylation sites at Ser^{45}, Ser^{102}, Ser^{120}, Thr^{169} and Ser^{210} (Figure 2).

A striking feature of the predicted $HRpI_{Cln}$ protein sequence, noted previously [23], is the abundance of negatively charged residues (24 % glutamic + aspartic residues); in particular, two clusters containing a high proportion of acidic residues are present between residues 97 and 107 (acidic domain I, 82 % acidic residues) and between residues 138 and 155 (acidic domain II, 67 % acidic residues) (Figure 2). Although the physiological significance of these acidic domains is unknown, the presence of acidic amino acid clusters is reminiscent of the RBC anion transporter, AE1 [11]. In human RBC AE1, the N-terminal cytoplasmic domain includes a stretch of 19 acidic residues within the first 40 residues and contains binding sites for many other proteins including haemoglobin, cytoskeleton proteins and enzymes [24].

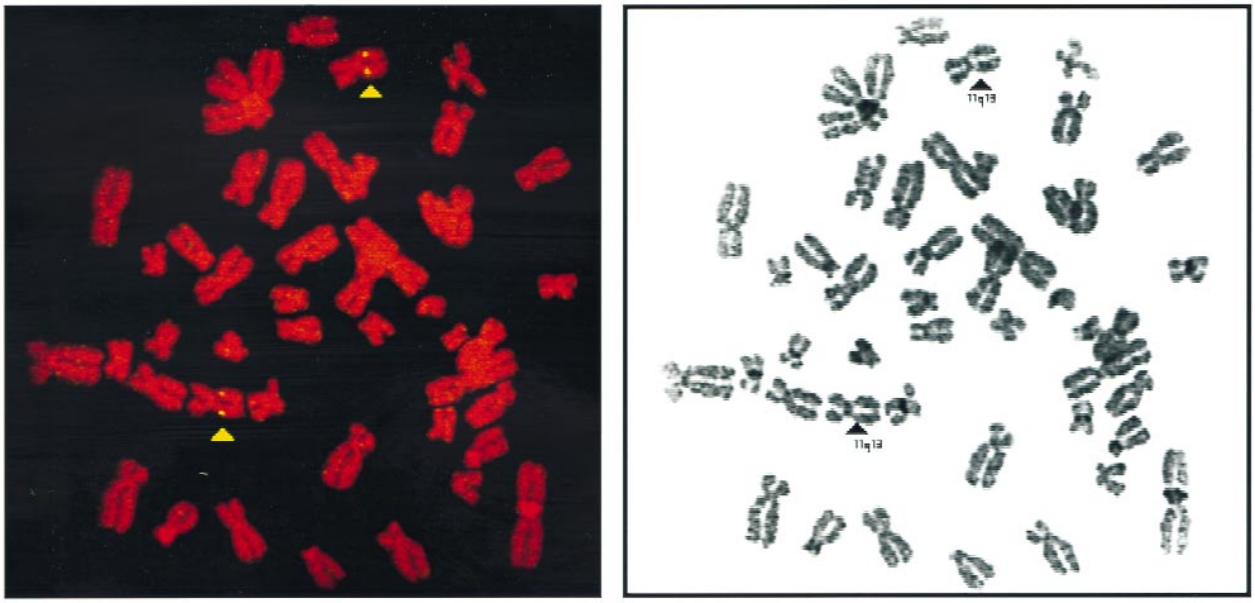

Figure 3 Chromosomal localization of the human I_{Cln} gene by FISH

Left panel: fluorescence image of normal human lymphocyte metaphase chromosome spread. Yellow signals denote hybridization loci of $HRpI_{Cln}$ probe (indicated by arrows). Chromosomes were counterstained with propidium iodide. Right panel: G-banded pattern of the same metaphase spread stained with Giemsa, localizing the human I_{Cln} gene to 11q13 (indicated by arrows).

Chromosomal localization

Using biotin-labelled full-length $HRpI_{Cln}$ cDNA (approx. 1.2 kb) to probe human metaphase-chromosome spreads, the location of the human I_{Cln} gene was mapped to 11q13 by FISH analysis (Figure 3). A database search of the NCBI Human Gene Map of 11q13 revealed that the domain identified by marker A006P03 (between D11S916 and D11S911, 80–84 cM) contained sequence strongly homologous to rat and dog pI_{Cln} (Genbank sequence names RNICLNA and CCCC respectively), thus confirming the FISH localization of the human I_{Cln} gene to 11q13 and further placing it within domain D11S916–D11S911.

Immunological identification and localization of $HRpI_{Cln}$

Polyclonal antibody to $HRpI_{Cln}$ detected two major bands in SDS/PAGE-separated human RBC ghost membranes at approx. 43 and approx. 37 kDa (Figure 4A, lane 1). The 43 and 37 kDa pI_{Cln} bands were similarly detected by polyclonal antibody to MDCK pI_{Cln} (aFPA [22]) (Figure 4A, lane 2), polyclonal antibody to rat C_6 glioma cell pI_{Cln} (Figure 4A, lane 4) and monoclonal antibody to MDCK pI_{Cln} (FChP12, [22]) (Figure 4A, lane 3). FChP12 also detected several minor bands migrating between 69 and 92.5 kDa (Figure 4A, lane 3). The 43 and 37 kDa pI_{Cln} bands were also detected by polyclonal antibody directed against a peptide containing residues 210–222 of rat pI_{Cln} (Figure 4B, lane 2) (rat pI_{Cln} sequence in [22]).

$HRpI_{Cln}$ bands were not detected in RBC haemolysates (results not shown), but this negative result does not exclude the possibility of the presence of some $HRpI_{Cln}$ in the cytosol because it might be difficult to detect in this compartment by virtue of its proportionally low content or increased susceptibility to proteolysis.

The 43 and 37 kDa $HRpI_{Cln}$ bands were found in both AA and SS ghost membranes, although the amount was considerably greater in SS ghosts (left panel of Figure 4C). As a 'loading' control, the same AA and SS ghosts were immunoblotted with polyclonal antibody to human RBC P4.2 [25], a component of the human RBC cytoskeleton whose 72 kDa isoform is known to be similar for both AA and SS RBC ghosts (A. C. Rybicki, unpublished work). As shown in the right panel of Figure 4(C), both AA and SS ghosts contained similar amounts of the P4.2 72 kDa isoform, demonstrating equivalent ghost protein loading. Because SS RBCs are much younger than AA RBCs [26,27] this opens up the possibility that the membrane content of $HRpI_{Cln}$ is dependent on cell age. This possibility is supported by a single experiment with RBCs from a patient with autoimmune haemolytic anaemia with 9.8% reticulocytes (see the Experimental section for clinical details), in which the membrane content of $HRpI_{Cln}$ was elevated compared with AA (results not shown).

Rabbit polyclonal anti-$HRpI_{Cln}$ antibody was used to immunolocalize the protein in methanol-fixed, acetone-permeabilized, AA RBCs. As shown in Figure 5 (top panels), low levels of $HRpI_{Cln}$ were detected in RBCs from unfractionated whole blood, as demonstrated by confocal laser scanning microscopy. Staining was concentrated in the membrane, with considerably less staining of the cytosol. The observed low level of cytosolic $HRpI_{Cln}$ fluorescence was probably not due to a loss of intracellular contents during fixation/permeabilization, because Giemsa-stained RBCs showed similar Hb staining whether the RBCs were fixed/permeabilized or air-dried without fixation/permeabilization (results not shown). Faint background fluorescence was observed with control non-immune IgG, most probably owing to Hb autofluorescence [28]. If the RBCs were not permeabilized, no specific fluorescence staining was detected with anti-$HRpI_{Cln}$ antibody (results not shown), suggesting that $HRpI_{Cln}$ either is not present exofacially, is unavailable to react with anti-$HRpI_{Cln}$ antibody, or the epitopes recognized by anti-$HRpI_{Cln}$ antibody are intracellular.

Because the level of $HRpI_{Cln}$ in SS ghost membranes was much higher than that in AA (Figure 4C), we examined a reticulocyte-enriched (young RBCs) density-fractionated subpopulation of

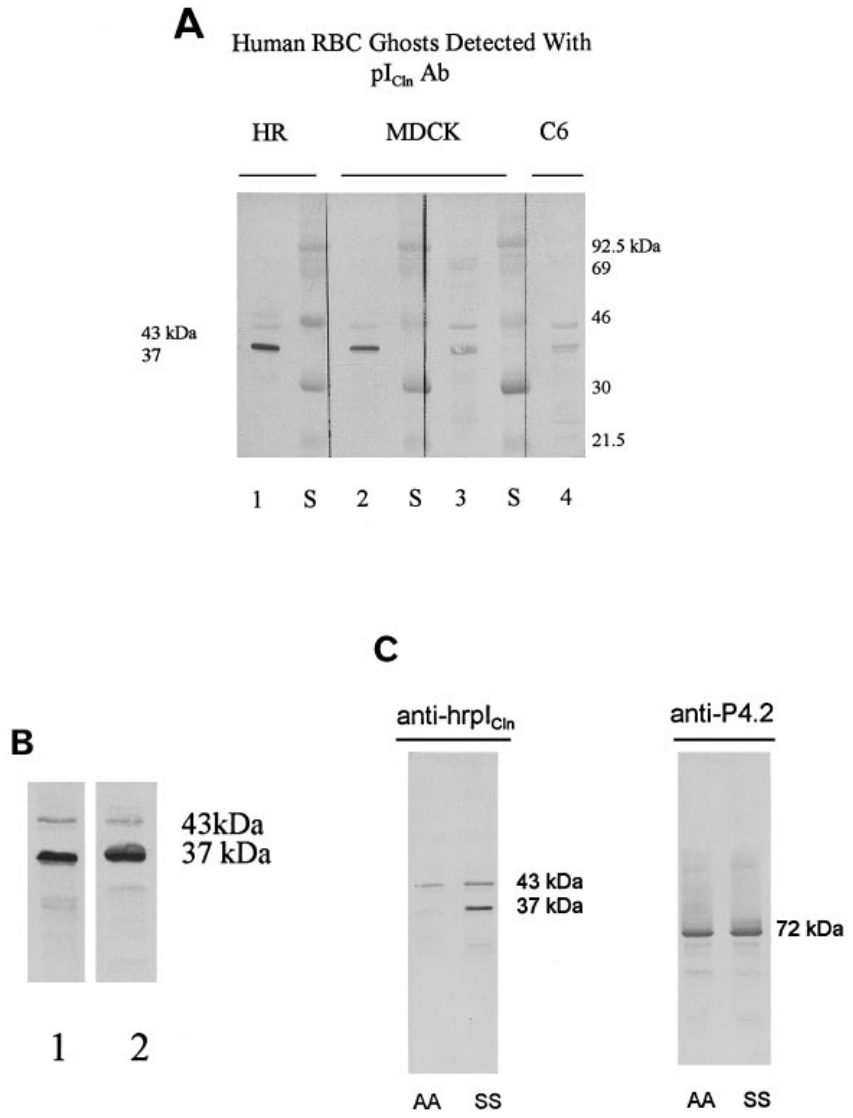

Figure 4 Western immunoblot of human RBC ghost membranes

(**A**) Ghosts (25 μg) from SS RBCs were separated by reducing SDS/PAGE and transferred electrophoretically to nitrocellulose as described in the legend to Figure 1. The nitrocellulose was probed with the following: lane 1, rabbit polyclonal anti-HRpI_{Cln} antibody (20 μg/ml); lane 2, rabbit polyclonal anti-(MDCK cell pI_{Cln}) antibody (4 μg/ml) [22]; lane 3, mouse monoclonal anti-(MDCK pI_{Cln}) antibody (18.5 μg/ml) (FChP12; [22]); lane 4, rabbit polyclonal anti-(C_6 glioma cell I_{Cln}) (1:50 dilution of antisera). Lanes S, prestained Amersham Rainbow protein molecular mass markers (RPN.756) (Arlington Heights, IL, U.S.A.). Molecular masses are shown at the right. Bound antibody was detected with alkaline phosphatase-conjugated second antibody and alkaline phosphatase colour reagents. (**B**) SS ghosts (25 μg) were subjected to SDS/PAGE and transferred electrophoretically to nitrocellulose as described in the legend to Figure 1. The nitrocellulose was probed with the following: lane 1, rabbit polyclonal anti-HRpI_{Cln} antibody (20 μg/ml); lane 2, rabbit polyclonal anti-rat pI_{Cln} peptide 210–222 antibody (5 μg/ml). (**C**) Left panel: as for (**A**) except that both normal (AA) and SS RBC ghosts were immunoblotted and probed with rabbit polyclonal anti-HRpI_{Cln} antibody (20 μg/ml). Right panel: as a sample 'loading' control, the same AA and SS ghosts were subjected to SDS/PAGE and transferred to nitrocellulose, which was probed with polyclonal antibody against human RBC P4.2 [25].

AA RBCs (less than 1.07 g/ml, equivalent to fraction 1) [13]. As shown in the bottom panels of Figure 5, the fluorescence staining intensity of HRpI_{Cln} in the young-cell, reticulocyte-enriched, AA fraction 1 was considerably greater than in unfractionated RBCs, consistent with the immunoblot results shown in Figure 4(C) and with the likely contention that the expression or membrane assembly of HRpI_{Cln} is dependent on cell age.

HR-pI_{Cln}-actin association *in vivo* detected by the yeast two-hybrid system

Krapivinsky et al. [22] reported that MDCK pI_{Cln} is capable of forming stable associations with actin *in vitro* and that a portion of isolated MDCK pI_{Cln} is bound to actin. This raised the interesting possibility that interactions between the cytoskeleton and MDCK pI_{Cln} might be involved in regulating pI_{Cln} activity. We found that anti-HRpI_{Cln} antibody co-immunoprecipitated soluble RBC β-actin, and that anti-β-actin antibody co-immunoprecipitated recombinant HRpI_{Cln} (results not shown). Moreover anti-β-actin antibody co-immunoprecipitated endogenous HRpI_{Cln} (low-salt extraction of SS RBC ghosts was the source of endogenous HRpI_{Cln}) (results not shown), further supporting earlier findings by Krapivinsky et al. [22] of pI_{Cln}-actin associations *in vitro*.

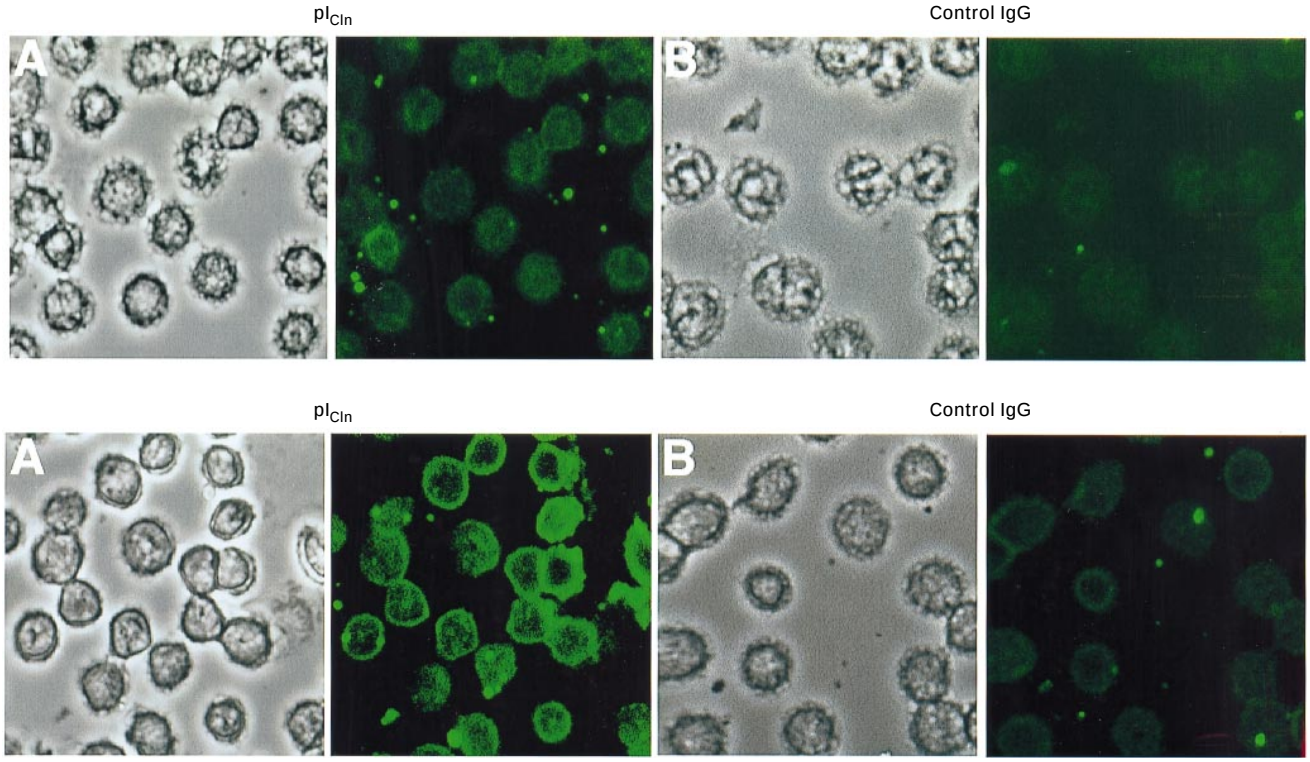

Figure 5 Localization of HRpI$_{Cln}$ in AA RBCs

Unfractionated RBCs from peripheral blood (top panel) or RBCs from a young cell-enriched fraction (bottom panel) (F1, equivalent to less than 1.07 g/ml [13]) were fixed with methanol, permeabilized with acetone and stained with either (**A**) polyclonal anti-HRpI$_{Cln}$ antibody or (**B**) non-immune (control) IgG. Bound IgG was detected by using biotin-conjugated anti-IgG and FITC-conjugated avidin. The left photograph of each pair is a phase-contrast image; the right photograph of each pair is the corresponding confocal laser scanning fluorescence image. Magnification $\times 1000$.

Table 2 Associations *in vivo* between HRpI$_{Cln}$ and β-actin demonstrated with the yeast matchmaker two-hybrid system 2

pCL1 encodes the full-length wild-type GAL4 protein and provides a positive control for the β-galactosidase assay. pAS2-1 and pACT2 are cloning vectors used to generate fusion proteins with the GAL4 DNA BD and AD respectively. pVA3-1 and pTD1-1 are DNA–BD and DNA–AD fusion plasmids respectively that provide a positive control for known interacting proteins (murine p53 and SV40 large T antigen respectively). pLAM5′-1 encodes a GAL4 DNA–BD/human lamin C fusion protein and provides a control for non-specific interactions. Numbers 1–13 are controls. Results for numbers 1 and 14 are from two separate clones.

Number	Plasmid 1 (DNA–BD)	Plasmid 2 (AD)	Yeast SD selection medium	LacZ phenotype (colony colour)	β-Galactosidase activity (units)
1	None	pCL1	−Leu	Blue	1061, 924
2	pAS2-1	None	−Trp	White	0
3	None	pACT2	−Leu	White	0
4	pAS2-1	pACT2	−Leu, −Trp	White	0
5	pVA3-1	None	−Trp	White	0
6	pVA3-1	pACT2	−Leu, −Trp	White	0
7	None	pTD1-1	−Leu	White	0.03
8	pAS2-1	pTD1-1	−Leu, −Trp	White	0.03
9	pVA3-1	pTD1-1	−Leu, −Trp	Blue	4.45
10	pLAM5′-1	None	−Trp	White	0.04
11	pLAM5′-1	pTD1-1	−Leu, −Trp	White	0
12	pAS2-1/HRpI$_{Cln}$	None	−Trp	White	0.02
13	None	pACT2/β-actin	−Leu	White	0
14	pAS2-1/HRpI$_{Cln}$	pACT2/β-actin	−Leu, −Trp	Blue	366, 357

To test for associations *in vivo* between HRpI$_{Cln}$ and β-actin we created fusion protein constructs containing full-length HRpI$_{Cln}$-DNA BD and full-length β-actin AD in expression plasmids provided by the manufacturer (Matchmaker kit; Clontech). These plasmids were used to transform yeast strain Y187, and transformants were selected and assayed for β-galactosidase activity. As shown in Table 2, in two separate clones, β-galactosidase activity was reconstituted in Y187 transformants containing both the HRpI$_{Cln}$-BD and β-actin-AD plasmids, but not in transformants lacking one or both plasmids.

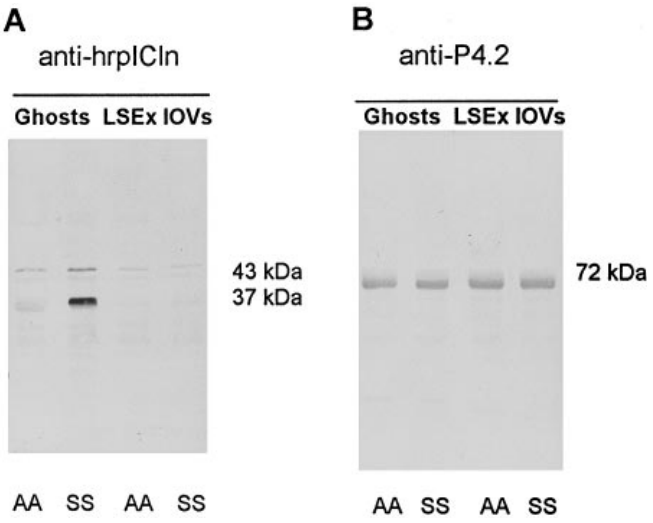

Figure 6 Extraction properties of RBC ghost $HRpI_{Cln}$

AA or SS ghosts were subject to low-salt extraction (LSEx) to strip off the spectrin–actin cytoskeleton [29]; the remnant inside-out vesicles (IOVs) were collected by centrifugation. Solubilized ghosts (25 μg) or SEx IOVs (25 μg) were subjected to reducing SDS/PAGE and transferred electrophoretically to nitrocellulose as described in the legend to Figure 1. (**A**) The nitrocellulose was probed with polyclonal anti-$HRpI_{Cln}$ antibody and developed as described in the legend to Figure 4. (**B**) Sample 'loading' control probed with human RBC anti-P4.2 antibody [25], as described in the legend to Figure 4(C).

Ghost membrane extraction properties of $HRpI_{Cln}$

We reasoned that if $HRpI_{Cln}$ and actin associate *in situ*, then the extraction of spectrin–actin from RBC ghost membranes by low-salt buffer should also extract $HRpI_{Cln}$. As shown in Figure 6, low-salt extraction of spectrin-actin from AA and SS RBC ghosts [29], which results in the formation of inside-out vesicles, also resulted in the almost complete extraction of $HRpI_{Cln}$.

DISCUSSION

Human young RBCs extrude K^+, Cl^- and water in response to acid/hypotonicity-induced cell swelling, eliciting an RVD and restoration of normal cell volume [1–3]. A major recognized RBC RVD transport system is the K:Cl co-transporter, which in addition to stimulation by cell swelling is also stimulated by cellular acidification ($pH \leqslant 7.0$) and thiol-modifying reagents [4,5]. K:Cl co-transport is only minimally expressed in mature circulating AA RBCs because its activity is cell age-dependent, but reticulocytes have a much higher K:Cl co-transport activity [6,9]. Moreover, a decrease in cell water content is a fundamental process of RBC maturation [30] and it is therefore possible that unrecognized volume-regulatory ion transport pathways could be important in erythropoiesis up to the young RBC stage.

Another potential candidate for an RBC RVD transport pathway is the swelling-induced Cl^- channel-associated protein pI_{Cln}, first described in MDCK cells [23] and later in many different cells and tissues [17,22,31], suggesting that it might be ubiquitously expressed. When overexpressed in *Xenopus* oocytes, pI_{Cln} allows a constitutively active, outwardly rectifying, external-Ca^{2+}-insensitive anion conductance that is partly inhibited by conventional anion channel inhibitors and strongly inhibited by Cl^- channel inhibitors [23]. It was later discovered that *Xenopus* oocytes have a native Cl^- current ($I_{Cl.swell}$) that is stimulated by hypotonicity-induced cell swelling, indistinguishable from the Cl^- current associated with overexpression of I_{Cln} [32]. Antibody to pI_{Cln} [22] or anti-sense oligonucleotides to I_{Cln} [33], injected into *Xenopus* oocytes, completely abolished $I_{Cl.swell}$, suggesting that pI_{Cln} was either directly responsible for $I_{Cl.swell}$ or regulated the activity of $I_{Cl.swell}$. Interestingly, in many cells expressing pI_{Cln}, as well as in *Xenopus* oocytes overexpressing MDCK I_{Cln}, the protein is most abundant in the cytosol [22]; thus it remains controversial whether pI_{Cln} is the actual Cl^- channel or a Cl^- channel regulator. Recent evidence in cultured NIH/3T3 fibroblasts that the cytosolic component of pI_{Cln} is driven into the membrane by exposing the cells to hypotonicity was used to support the contention that pI_{Cln} is a Cl^- channel in these cells [34].

From the use of oligonucleotide primers derived from NPE pI_{Cln} cDNA [17], we report here the cloning from human reticulocyte cDNA a sequence whose ORF is identical with that of NPE pI_{Cln}. By using full-length $HRpI_{Cln}$ cDNA (approx. 1.2 kb) to probe human lymphocyte metaphase-chromosome spreads, the location of the human I_{Cln} gene was mapped to 11q13 by FISH analysis. Polyclonal anti-$HRpI_{Cln}$ antibody recognized two major bands at approx. 43 kDa and approx. 37 kDa in solubilized AA and SS RBC ghost membranes, although the amount of protein is greater in SS ghosts. It is likely that both the 43 and 37 kDa bands correspond to pI_{Cln} because monoclonal anti-MDCK antibody, and antibody directed against a C-terminal peptide (residues 210–222) of rat pI_{Cln} [22], recognized both bands.

The reason for the discrepancy between the predicted $HRpI_{Cln}$ molecular mass (approx. 26 kDa), and the observed 43 kDa and 37 kDa bands in RBC ghost membranes by SDS/PAGE is unknown. A similar discrepancy between MDCK pI_{Cln} predicted molecular mass (approx. 26 kDa) and that of native, or *in vitro* translated, MDCK pI_{Cln} (37 kDa) has previously been noted [22,23]. We do not currently have evidence for $HRpI_{Cln}$ mRNA splicing isoforms, although this negative result does not exclude that possibility. It should be noted that endogenous pI_{Cln} in *Xenopus* oocytes migrates as a 41 kDa [22] or 43 kDa [35] band on SDS/PAGE, despite having a nearly identical number of acidic amino acid residues to those in MDCK pI_{Cln}, which migrates at 37 kDa [22]; also, in *Xenopus* oocytes overexpressing MDCK pI_{Cln} both 37 kDa and 43 kDa pI_{Cln} bands are observed [22]. The molecular mechanisms responsible for the different mobilities on SDS/PAGE of these pI_{Cln} bands is unknown.

$HRpI_{Cln}$ is located predominantly in the plasma membrane, in contrast with the cellular location of MDCK, NIH/3T3 and *Xenopus* oocyte pI_{Cln}, which is most abundant in the cytosol (reviewed in [31]). Fluorescent staining was much greater in a young AA RBC population than in unfractionated AA RBCs, which are predominantly mature RBCs. Taken together with the increased content of $HRpI_{Cln}$ in SS ghost membranes, these results suggest that the expression or membrane assembly of $HRpI_{Cln}$ is developmentally regulated. This possibility was previously suggested for the human RBC K:Cl co-transporter [9].

Evidence for associations *in vivo* between $HRpI_{Cln}$ and β-actin was obtained by using the yeast two-hybrid system. Fusion proteins containing GAL4-BD–$HRpI_{Cln}$ and GAL4-AD–β-actin expressed together in yeast reconstituted GAL4 function and resulted in the expression of a reporter gene. These results suggest that $HRpI_{Cln}$ and β-actin are capable of forming stable associations *in vivo*.

$HRpI_{Cln}$ is extracted from RBC ghost membranes under low-ionic-strength conditions that also result in the extraction of the spectrin–actin cytoskeleton. These results are consistent with the evidence for pI_{Cln}–actin association *in vitro* ([21], and R. S. Schwartz and A. C. Rybicki, unpublished work) and *in vivo* (our

yeast two-hybrid results). However, another possible interpretation of the extraction data is that $HRpI_{Cln}$ is membrane-associated but not membrane-bound, because it is easily extracted; this is a possibility more compatible with $HRpI_{Cln}$'s being a Cl^- channel regulator than its being a Cl^- channel.

If $HRpI_{Cln}$ and RBC actin associate intracellularly, this raises the interesting possibility that the cytoskeleton could participate in the regulation of $HRpI_{Cln}$ activity. A role for the cytoskeleton in regulating erythroid RVD has been previously proposed on the basis of the following evidence: (1) inhibitors of actin polymerization cause partial loss of swelling-induced K:Cl co-transport activation in human RBCs [36], and (2) heating rat RBCs to temperatures where spectrin thermal denaturation begins blocks the swelling-induced activation of K:Cl co-transport [37]. These results are largely phenomenological; the demonstration of a direct role of the cytoskeleton in regulating erythroid RVD remains at present an alluring possibility.

Our finding of $HRpI_{Cln}$ in human RBCs does not define its function; indeed we do not have any evidence that this protein is involved in RBC Cl^- transport or RVD. However, that pI_{Cln} in other cells [22,23], including human cells [17,35], is involved in Cl^- transport and RVD, suggests that $HRpI_{Cln}$ is a candidate protein for these functions in young or immature RBCs.

We thank Dr. G. B. Krapivinsky for providing polyclonal and monoclonal anti-MDCK pI_{Cln} antibody and polyclonal anti-rat pI_{Cln} 210-222 peptide antibody, and for helpful discussions; Dr. L. A. Cannizzaro and M. Zohouri for chromosomal FISH analysis; Dr. K. Strange for providing anti-C_6 glioma cell pI_{Cln} antiserum, and for helpful discussions; and S. Musto for technical assistance. This work was supported in part by grant HL38655 (to R.S.S.; Project 2) from the National Institutes of Health.

REFERENCES

1 Agre, P. and Parker, J. C. (1989) Red blood cell membranes: structure, function, clinical implications, Marcel Dekker, New York
2 Brugnara, C. (1993) Experientia **49**, 100–109
3 Joiner, C. H. (1993) Am. J. Physiol. **264**, C251–C270
4 Lauf, P. K., Bauer, J., Adragna, N. C., Fujise, H., Zade-Oppen, A. M., Ryu, K. H. and Delpire, E. (1992) Am. J. Physiol. **263**, C917–C932
5 Brugnara, C. and Tosteson, D. C. (1987) Am. J. Physiol. **252**, C269–C276
6 Hall, A. C. and Ellory, J. C. (1986) Biochim. Biophys. Acta **858**, 317–320
7 Brugnara, C., Bunn, H. F. and Tosteson, D. C. (1986) Science **232**, 388–390
8 Canessa, M., Spalvin, A. and Nagel, R. L. (1986) FEBS Lett. **200**, 197–120
9 Canessa, M., Fabry, M. E., Blumenfeld, N. and Nagel, R. L. (1987) J. Membr. Biol. **97**, 97–105
10 Hoffmann, E. K. and Dunham, P. B. (1995) Int. Rev. Cytol. **161**, 173–262
11 Tanner, M. J. A. (1993) Semin. Hematol. **30**, 34–57
12 Jennings, M. L. (1992) in The Kidney: Physiology and Pathophysiology, 2nd edn., (Seldin, D. W. and Giebish, G., eds.), pp. 503–535, Raven Press, New York
13 Fabry, M. E. and Nagel, R. L. (1982) Blood Cells **8**, 9–15
14 Dodge, J. T., Mitchell, C. and Hanahan, D. J. (1963) Arch. Biochem. Biophys. **100**, 119–130
15 Glader, B. E. (1994) in Sickle Cell Disease: Basic Principles and Clinical Practice, (Embury, S. H., Hebbel, R. P., Mohandas, N. and Steinberg, M. H., eds.), pp. 545–554, Raven Press, New York
16 Temple, G. F., Chang, J. C. and Kan, Y. W. (1977) Proc. Natl. Acad. Sci. U.S.A. **74**, 3047–3051
17 Anguita, J., Chalfant, M. L., Civan, M. M. and Coca-Prados, M. (1995) Biochem. Biophys. Res. Commun. **208**, 89–95
18 Shi, G. and Cannizzaro, L. A. (1996) Cytogenet. Cell Genet. **75**, 180–185
19 Guan, K. L. and Dixon, J. E. (1991) Anal. Biochem. **192**, 262–267
20 Laemmli, U. K. (1970) Nature (London) **227**, 680–685
21 Towbin, H., Staechelin, T. and Gordon, J. (1979) Proc. Natl. Acad. Sci. U.S.A. **76**, 4350–4354
22 Krapivinsky, G. B., Ackerman, M. J., Gordon, E. A., Krapivinsky, L. D. and Clapham, D. E. (1994) Cell **76**, 439–448
23 Paulmichl, M., Li, Y., Wickman, K., Ackerman, M., Peralta, E. and Clapham, D. (1992) Nature (London) **356**, 238–241
24 Low, P. S. (1986) Biochim. Biophys. Acta **864**, 145–167
25 Rybicki, A. C., Heath, R., Wolf, J. L., Lubin, B. and Schwartz, R. S. (1988) J. Clin. Invest **81**, 893–901
26 McCurdy, P. R. and Sherman, A. S. (1978) Am. J. Med. **64**, 253–258
27 Serjeant, G. R., Serjeant, B. E. and Milner, P. F. (1969) Br. J. Haematol. **17**, 527–553
28 Hirsch, R. E. (1994) Methods Enzymol. **232**, 231–246
29 Fairbanks, G., Steck, T. L. and Wallach, D. F. H. (1971) Biochemistry **10**, 2606–2617
30 Sieff, C. A. and Williams, D. A. (1995) in Blood: Principles and Practice of Hematology (Handin, R. I., Lux, S. E. and Stossel, T. P., eds.), pp. 171–224, JB Lippincott, Philadelphia
31 Strange, K., Emma, F. and Jackson, P. S. (1996) Am. J. Physiol. **270**, C711–C730
32 Ackerman, M. J., Wickman, K. D. and Clapham, D. E. (1994) J. Gen. Physiol. **103**, 153–179
33 Gschwentner, M., Nagl, U. O., Woll, E., Schmarda, A., Ritter, M. and Paulmichl, M. (1995) Eur. J. Physiol. **430**, 464–470
34 Paulmichl, M., Gschwentner, M., Nagl, U. O., Filrst, H., Woll, E., Laich, A., Rovan, E., Susanna, A., Dobson, A., Schmarda, A., Pringgers, G. and Leitinger, M. (1995) Biophys. J. **68**, 242 (Abstract)
35 Buyse, G., De Greef, C., Raeymaekers, L., Droogmans, G., Nilius, B. and Eggermont, J. (1996) Biochem. Biophys. Res. Commun. **218**, 822–827
36 Garay, R. P., Nazaret, C., Hannaert, P. A. and Cragoe, E. J. (1988) Mol. Pharmacol. **33**, 696–701
37 Orlov, S. N., Kolosova, I. A., Cragoe, E. J., Gurlo, T. G., Mongin, A. A., Aksentsev, S. L. and Konev, S. V. (1993) Biochim. Biophys. Acta **1151**, 186–192

Received 5 December 1996/6 May 1997; accepted 9 June 1997